Progress in Propulsion Physics **2** (2011) 617-628
© Owned by the authors, published by EDP Sciences, 2011

INVESTIGATION OF DISCHARGE CHANNEL WALL MATERIAL INFLUENCE ON LIFETIME OF HALL EFFECT THRUSTER WITH HIGH SPECIFIC IMPULSE

V. V. Abashkin, M. B. Belikov, O. A. Gorshkov, A. S. Lovtsov, and I. N. Khrapach

Keldysh Research Center
Onezhskaya Str. 8, Moscow 125438, Russia

Results of 500-hour life tests of the 900-watt Hall-thruster laboratory model with the specific impulse of 2000 s are presented. The thruster discharge channel walls were manufactured from 60% BN + 40% SiO_2 and > 90% BN hot-pressed ceramics. The predicted total lifetime was ∼ 3000 h for both wall materials in spite of greater erosion resistance of pure BN in comparison with BN–SiO_2 mixture. To clarify the accompanying phenomena, the following diagnostics were carried out. The surface microstructure and composition insulators were investigated by means of electron microscopy and X-ray fluorescence analysis and near-wall plasma parameters were measured with flat Langmuir probes. The obtained distributions of plasma parameters were compared with the results of stationary one-dimensional (1D) hydrodynamic modeling of discharge channel.

1 INTRODUCTION

Recent trends in commercial spacecraft development increased requirements to Hall effect thrusters (HET) used in orbit correction propulsion systems in terms of specific impulse and lifetime. In particular, the total specific impulse has to be increased up to 3000 s with the lifetime more than 7000 h. To satisfy these requirements, the existing HET models with space flight experience should be modified. In general, it is necessary to change discharge chamber geometry, magnetic field topology inside the discharge channel, and materials of discharge channel walls.

This is an Open Access article distributed under the terms of the Creative Commons Attribution-Noncommercial License 3.0, which permits unrestricted use, distribution, and reproduction in any noncommercial medium, provided the original work is properly cited.

Article available at http://www.eucass-proceedings.eu or http://dx.doi.org/10.1051/eucass/201102617

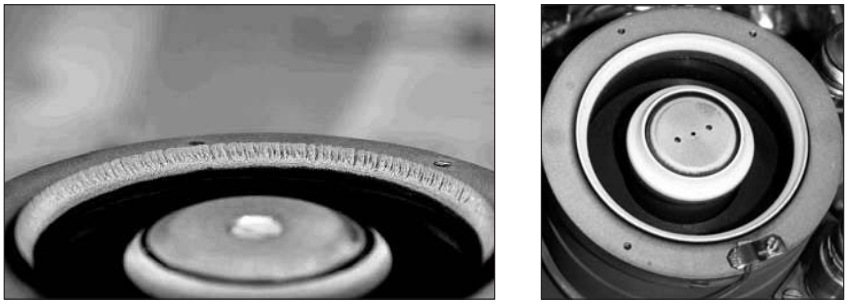

(*a*) (*b*)

Figure 1 The 900-watt HET after 500 h of operation at discharge voltage 500 V: (*a*) BGP walls; and (*b*) BN-05 walls

The discharge channel walls of HETs used in space missions today are made of BGP — a ceramic material consisting of $\sim 60\%$ BN and $\sim 40\%$ SiO_2. Despite this material provides excellent mechanical and insulating properties, its sputter resistance to xenon plasma is hampered by relatively high fraction of SiO_2 [1]. New materials with enhanced erosion resistance and output parameters comparable to those for HET with BGP are searched in various laboratories [2–4]. Experiments conducted in Keldysh Center and other laboratories show that boron nitride of high purity (more than 90%) is to be considered as the most promising substitute for BGP.

Within the frame of work presented in this paper, a hot-pressed hexagonal boron-nitride ceramic (h-BN) with less than 4% boron oxide and calcium oxide used as binders (named BN-05) was studied along with BGP as materials for HET discharge-channel walls. The laboratory model of HET with power of 900 W and specific impulse of 2000 s was equipped with insulators made of both ceramics and 500-hour life tests were carried out for each material [5]. The specific impulse degradation during life tests was 100 s lower for BN-05 walls than for the BGP ones. The full lifetime predicted with a semiempirical model [6] for both materials was ~ 3000 h.

Obvious causes of observed phenomena, namely, similarity of sputtering yields for both materials and differences in discharge-channel walls macrostructure were considered in [5]. It was shown that BN-05 had a sputter yield a factor of 1.5–2 less than BGP in the range of Xe ions energy 250–500 eV and in the range of ion beam incidences 0°–70°. Furthermore, it was shown that during first 500 h of operation, "anomalous erosion" structure appeared on the BGP walls while BN-05 wall surface remained relatively smooth (Fig. 1).

The objective of this paper was to clarify the physical mechanism beyond the similarity of lifetime for Hall thrusters with different sputter-resistant discharge-channel wall materials. The wall surface microstructure and composition of

different HETs developed in Keldysh Center were investigated and near-wall plasma parameters were measured for BGP and BN-05 walls.

A simple 1D stationary hydrodynamic model of Hall thruster plasma in the discharge chamber was developed to explain the results obtained.

2 WALL SURFACE MICROSTRUCTURE AND COMPOSITION INVESTIGATION

The wall surface was investigated using two diagnostics: Environmental Scanning Electron Microscopy (ESEM) method, which allowed studying insulating ceramics without deposition of any conductive coating, and conventional X-ray Fluorescence Spectroscopy (XRFS) analysis. Due to the relatively low mass of atoms composing the ceramics under study and small scale of considered microstructures, the results of XRFS are qualitative whereas ESEM pictures are considered as a reliable source of quantitative information.

It is well known [7] that during prolonged operation of HET with BGP discharge-channel walls, two kinds of macrostructures appear on the insulators surface at discharge voltage 300–350 V. The first with regular peaks and holes referred to as normal erosion and the second with periodic grooves oriented axially at the cathode side of walls referred to as anomalous erosion. The normal erosion structure appears after 5–10 h of operation. Similar structure appears during ceramic sample sputtering in the plume of a Kaufman plasma source or a HET [1, 5]. It was proposed [1] that normal erosion is caused by differences in sputtering yields of BN and SiO_2 grains of BGP. While physical mechanism beyond the anomalous erosion is not so clearly understood, the appearance of anomalous erosion structures is the important indicator of HET operation mode. Usually, it is connected with major decrease of channel-wall sputtering rate [7]. Both normal and anomalous erosion structures were observed on the walls of the tested HET laboratory model made of BGP after 500 h of operation in a high specific impulse mode. The ESEM images of these structures are presented in Fig. 2*a* and 2*b*.

The XRFS analysis showed that material composition at the top of normal erosion peaks and anomalous erosion grooves was generally similar to composition of nonsputtered material (B, N, Si, and O atoms). The bottom of normal erosion holes usually consisted of Si and O atoms. The walls of holes were often covered with scales composed of the material redeposited from its bottom. The anode side of discharge channel walls was covered with dark-brown and black films composed, mainly, of Si and O with traces of B, N, C, Al, Fe, and Xe atoms.

At greater level of magnification, the “fine structure” of normal and anomalous erosion patterns was detected on BGP walls. This structure consisted of

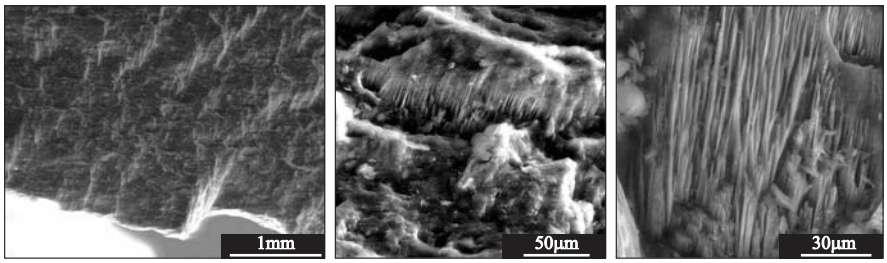

(*a*) (*b*) (*c*)

Figure 2 The ESEM results for BGP wall structure at different magnification levels: (*a*) anomalous erosion structure (element size $\sim$ 1 mm); (*b*) normal erosion (element size $\sim$ 150 μm); and (*c*) needles of "fine structure" (diameter 50–600 nm, length 100–1600 nm)

needles 50–600 nm in diameter and 100–1600 nm long (Fig. 2*c*). Erosion "fine-structure" needles were located at the sides of anomalous and normal erosion elements covered due to direct HET plasma plume bombardment, i. e., generally, at the cathode-oriented side of these structures. There were no such structures observed on the samples sputtered in the HET plasma plume. So, it was supposed that these needles appeared due to plasma-enhanced redeposition of sputtered material from one channel wall to another. The intensity of Si and O atoms radiation lines in the XRFS spectra of these needles was much greater than in the spectrum of unsputtered material.

The presented results of XRFS and ESEM analyses showed that BGP wall structure and composition change greatly with HET lifetime. These changes should be considered during HET modeling and development. A possible mechanisms of "fine structure" influence on the HET operation require detailed investigation. At the first glance, such structures can affect transportation of plasma electrons through changes in wall emissivity properties.

The typical structure of 900-watt thruster BN-05 wall obtained by ESEM is presented in Fig. 3*a*. As one can see, the structure consists of flat grains bound together, with thin edges oriented normally to the picture plane. The size of observed grains is close to the size of h-BN powder particles used for manufacturing the BN-05 ceramics. The axis of hot pressing was oriented from the top of the figure to its bottom. The XRFS analysis of BN-05 wall structure did not show any radical changes in material composition in comparison with unsputtered material.

To find out the reasons for the lack of anomalous erosion structures on the 900-watt HET model walls, another HET model — KM-32 — equipped with BN-05 walls was investigated with the ESEM method. The KM-32 thruster was designed for operation in power range 100–300 W, discharge voltage range 250–

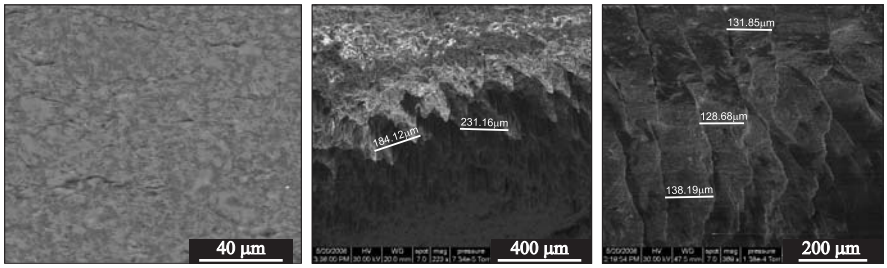

(*a*) (*b*) (*c*)

Figure 3 The ESEM results for BN-05 and BGP wall structure in different HETs: (*a*) 900-watt HET, discharge voltage 500 V, BN-05 walls, lifetime 500 h, normal erosion elements (size $\sim$ 3–5 μm); (*b*) KM-32, discharge voltage 250 V, BGP walls, lifetime 180 h, first appearance of anomalous erosion structure (period $\sim$ 200–250 μm); and (*c*) KM-32, discharge voltage 250 V, BN-05 walls, lifetime 500 h, anomalous erosion structure (period $\sim$ 200–250 μm)

400 V, and successfully passed 180-hour life test with BGP walls and 500-hour life test with BN-05 walls [8]. The results of ESEM for the outer wall of KM-32 are presented in Figs. 3*b* and 3*c*. The anomalous erosion structure can be clearly seen in both figures; however, on BN-05 walls, the structure appeared 200–250 h later than on the BGP walls. The structure period was of similar size ($\sim$ 200 μm) for both materials.

The phenomenon of late appearance of anomalous erosion on BN-05 walls in comparison with BGP can be caused by the differences in the intensity of normal erosion for the investigated materials, while anomalous erosion is quite similar in intensity and resulting structure composition [7].

3 MEASUREMENTS OF NEAR-WALL PLASMA PARAMETERS

The first results of analysis of near-wall plasma parameters for the 900-watt HET laboratory model under investigation were reported in [5]. However, the values of ion current on the walls were estimated with several assumptions proved to be erroneous for high-voltage modes of HET operation for probes located in the acceleration zone, i. e., in the area where the plasma potential drop was observed. The measured values of plasma potential were also overestimated. The analysis of the data obtained and systematic errors observed led to the following conclusions: the temperature of electrons could be measured with a lower error, following by the floating and plasma potentials. The absolute values

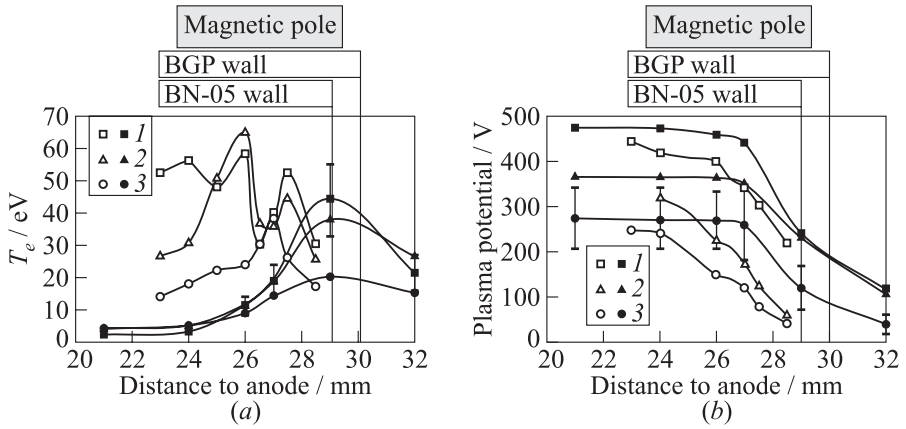

Figure 4 Distributions of plasma parameters in the 900-watt HET laboratory model (empty signs — BN-05 and filled signs — BGP) at different discharge voltages (*1* — 500 V; *2* — 400; and *3* — 300 V) and anode mass flow rate of 1.8 mg/s: (*a*) electron temperature; and (*b*) plasma potential

of electron and ion currents were measured with the greatest errors and could be considered only as auxiliary qualitative data. Based on these conclusions, the following experiments were performed.

Flat Langmuir probes were installed into the outer discharge channel walls to obtain distributions of local plasma parameters for the 900-watt HET laboratory model equipped with BN-05 and BGP walls. The volt-ampere characteristics of the probes were collected after 3 h of HET operation at a chosen mode. The power source allowed rapid decrease of probe voltage from the level 50 V higher than plasma potential to the ground potential. The signal from the probe was visualized using the recording oscilloscope and the volt-ampere characteristic was chosen for further manual processing. The value of floating potentials for all probes was continuosly controlled during the experiment.

The measurement error was estimated as 25%–30%. It included the errors due to changes of probe geometry during the measurements, uncertainty of probe positioning relatively to the wall inner surface, non-Maxwellian electron energy distribution, and periodic changes of plasma parameters during the experiment.

The distributions of electron temperature for different operation modes are presented in Fig. 4*a*. The corresponding distributions of plasma potential are presented in Fig. 4*b*. Positions of outer magnetic pole and outer discharge channel wall are also presented in the figures.

The cause of the two-hump electron temperature distribution in case of BN-05 walls is unclear. One can see that the areas of the maximum electron temperature

and electric field are located 1–1.5 mm closer to the anode in case of BN-05 walls. The maximum of electron temperature is higher for BN-05 walls, which corresponds to the results published in [9].

Based on the presented data, one can presume that ionization and acceleration zones for BN-05 walls are located closer to the anode than those for BGP walls. Thus, the mean energy of ions bombarding BN-05 walls should be higher than in the case of BGP walls as well as ion current density. This phenomenon is recognized as the main cause of equal lifetime for both materials.

4 ONE-DIMENSIONAL MODEL OF DISCHARGE CHAMBER

To obtain the quantitative dependence of axial position of ionization and acceleration zones on the wall properties, a simple 1D stationary model was developed. The approach was similar to that used in [10]. Plasma of discharge channel of height h and cross-section area S was modeled. The model included the following plasma components: electrons, single charged ions, and neutral atoms. The processes of elastic electron–neutral scattering, inelastic electron–neutral excitation, electron–neutral ionization, ions loss to the wall, and electron energy loss to the wall due to collisions were modeled. The neutrals were injected through the anode-side of the model region. Their temperature and velocity were assumed to be constant. All mentioned collisions were modeled by the appropriate frequencies:

$$\left.\begin{aligned} \nu_{iw} &= \alpha_w \frac{1}{h} \cdot 2 \frac{1}{n_i} \Gamma_i \,; \\ \nu_{ew} &= \alpha_w \frac{1}{h} \cdot 2 \frac{1}{n_e} \Gamma_e \,; \\ \nu_i &= n_n \sigma_i \left(\frac{8kT_e}{\pi m} \right)^{1/2} \left(1 + 2 \frac{kT_e}{E_i} \right) \exp\left(-\frac{E_i}{kT_e} \right) \,; \\ \nu_n &= n_n \sigma_n \left(\frac{8kT_e}{\pi m} \right)^{1/2} \end{aligned}\right\} \tag{1}$$

where m is the electron mass; ν_{iw} is the frequency of ion loss to walls; ν_{ew} is the frequency of electron collisions with walls; ν_i is the frequency of ionization; ν_n is the frequency of elastic collisions of electrons with neutrals; $\alpha_w = 0.3 \ldots 0.003$ is the attenuation coefficient introduced for taking magnetic confinement of electrons between walls into account; $\sigma_n = 2.7 \cdot 10^{-19}$ is the mean cross section of elastic electron–neutrals collisions; $\sigma_i = 3.6 \cdot 10^{-20}$ is the mean ionization cross section; T_e is the electron temperature; $E_i = 12.1$ eV is the ionization potential

of Xe; Γ_i and Γ_e are the ion and electron fluxes to the walls; and n_n, n_e, and n_i are the concentrations of neutrals, electrons, and ions.

Near-wall potential drop φ_w was calculated according to [11]:

$$\varphi_w = \begin{cases} -\dfrac{kT_e}{e}\left(\dfrac{1}{2}\ln\left(\dfrac{MT_e}{mT_i}\right) + \ln(1-\delta)\right) & \text{if } \delta < 0.997\,; \\ -\dfrac{kT_e}{e} & \text{if } \delta \geq 0.997 \end{cases} \tag{2}$$

where e is the electron charge; and δ is the integral yield of secondary electrons.

For δ, the exponential approximation was used:

$$\delta(\varepsilon) = \left(\frac{\varepsilon}{\varepsilon_1}\right)^{\alpha} \tag{3}$$

where ε is the total kinetic energy of electrons; and ε_1 (31 eV for BN-05 and 53 eV for BGP [12]) and α (0.57 for BN-05 and 0.64 for BGP [12]) are the constants.

Ion flux to the wall equaled electron flux to the wall with the deduction of the flux of secondary electrons:

$$\Gamma_i = \begin{cases} \Gamma_e(1-\delta) = \left(\dfrac{kT_e}{2\pi m}\right)^{1/2} n_e \exp\left(\dfrac{e\varphi_w}{kT_e}\right)(1-\delta) & \text{if } \delta < 0.997\,; \\ \Gamma_e = \left(\dfrac{kT_e}{2\pi m}\right)^{1/2} n_e & \text{if } \delta \geq 0.997 \end{cases} \tag{4}$$

where $T_i = T_n = 1000$ K are the temperatures of ions and neutrals and M is the xenon atom mass.

This way, a possibility of occurrence of charge saturation (SCS) mode was taken into account.

The conservation equations of ion mass and momentum were solved for a given electron temperature and magnetic field distribution inside the discharge chamber:

$$\frac{d\left(n_i V_i\right)}{dz} = n_e\nu_i - n_i\nu_{iw}\,; \tag{5}$$

$$\frac{d\left(n_i {V_i}^2\right)}{dz} = \frac{e}{M} n_e E + n_e\nu_i V_n - n_i\nu_{iw} V_i. \tag{6}$$

The motion equation of electrons was reduced to

$$V_e = -\left(\frac{e}{m}\left[\frac{\nu_n + \nu_{ew}}{\Omega_e^2}\right] + \frac{\alpha_A}{B}\right) E = -\mu_e E \tag{7}$$

where μ_e is the axial mobility of electrons; E is the electric field; V_e is the electron axial velocity; B is the magnetic field; $\Omega_e = eB/m_e$ is the electron cyclotron frequency; and $\alpha_A = 1/160$ is the coefficient of anomalous diffusion of electrons.

Equations of discharge-current continuity, heavy-particles global mass continuity, and plasma quasi-neutrality were also solved:

$$I_d = const = eS(n_e V_e + n_i V_i)\,; \quad n_n V_n + n_i V_i = const = \frac{\dot{m}_a}{MS}\,; \quad n_e = n_i \quad (8)$$

where I_d is the discharge current; $V_n = const = ((5/3)(kT_n)/M)^{1/2}$ is the neutral velocity; and $\dot{m}_a$ is the anode mass flow rate, kg/s.

The initial degree of ionization was assumed equal to 0.01. To determine the physical mechanism of experimentally observed difference in the acceleration zone position, the distribution of electron temperature was taken equal for both

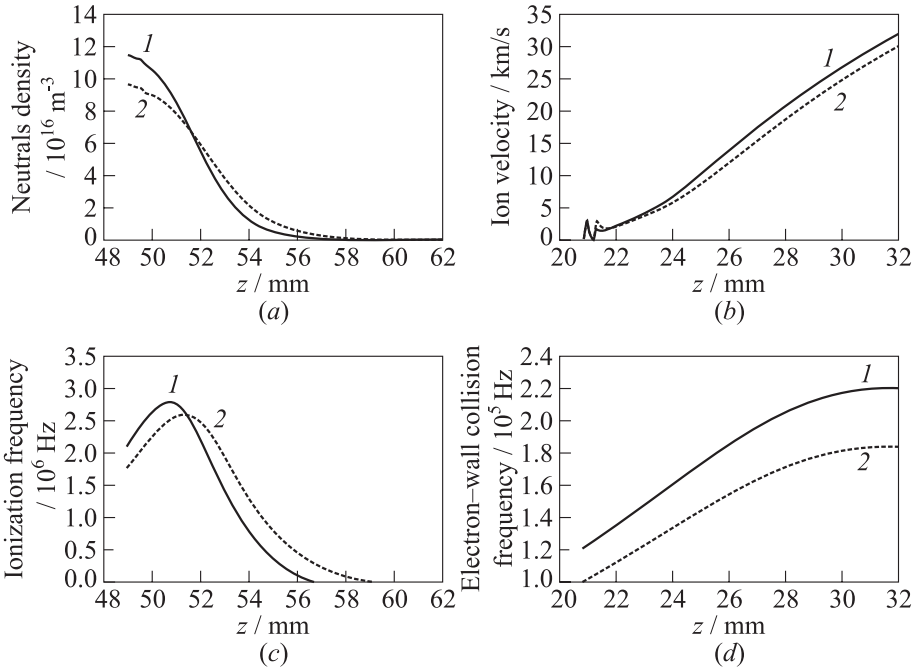

Figure 5 Results of calculations for axial distributions of plasma parameters (I_d = 1.8 A, $\dot{m}_a = 2.11 \cdot 10^{-6}$ kg/s, $T_{e_{\max}} = 50$ eV): (*a*) neutrals density; (*b*) ion velocity; (*c*) ionization frequency; and (*d*) electron–wall collision frequency (*1* — BN and *2* — BGP)

materials and close to that measured experimentally for BGP. The results of numerical integration of Eqs. (1)–(8) are presented in Figs. 5*a*–5*d*.

Despite simplicity of the proposed model, the results of calculations allowed to reveal the difference in the ionization zone position and the conditions of ion acceleration. The difference was caused by the realization of the SCS mode in case of BN-05 walls, while in case of BGP walls, this mode was not realized. Significant difference in electron–wall collision frequency for BGP and BN-05 (see Fig. 5*d*) caused the increase of electron conductivity in the latter case, shift of ionization frequency, and electric-field maximum to the anode. Varying initial T_e distribution, one could realize SCS mode for both materials or for none.

If the SCS mode was not realized, then the differences in the axial positions of ionization and acceleration zones were similar to Fig. 5. If the SCS mode was realized for both materials, then the ionization and acceleration zones of BN-05 and BGP became indistinguishable.

Today, the described model is not a reliable instrument for calculating the self-consistent plasma parameters of HET. There are nonrealistic oscillations of ion velocities in the anode-side of the modeled area, and the obtained value of plasma potential drop inside the channel is too large in comparison with that measured experimentally. To improve the model, it is needed to include in the calculations the electron heat balance equation, to determine a_w using the results of two-dimensional modeling of magnetic field, and to model realistic velocity and density distribution of neutrals.

5 CONCLUDING REMARKS

The results of 500-hour life tests of 900-watt Hall-thruster laboratory model with the specific impulse of 2000 s and discharge channel walls made of BN-05 and BGP ceramics are reported. The application of more sputter-resistant material as an insulator did not increase HET total lifetime. In this paper, possible reasons of the observed lifetime similarity in terms of differences in wall surface morphology and composition and dependence of near-wall plasma parameters on wall material properties were descussed.

The wall surfaces were investigated using ESEM method and conventional XRFS analysis. Atomic composition of different parts of BGP and BN-05 walls was investigated.

It was shown that besides well-known normal and anomalous erosion structures, the “fine structure” composed of needles 50–600 nm in diameter and 100–1600 nm long existed on BGP walls after 500 h of HET operation. It was also shown that the anomalous erosion structure could appear both on BN-05 and BGP walls. The period of the initial grooves looked similar, while their appearance on BN-05 walls was 200–250 h later than on the BGP walls.

Near-wall distributions of plasma parameters were measured for both wall materials using flat Langmuir probes. The areas of maximum electron temperature and electric field were shown to locate 1–1.5 mm closer to the anode in case of BN-05 walls. It was proposed that this phenomenon was responsible for the lifetime similarity obtained for the 900-watt Het laboratory model with BN-05 and BGP walls.

To obtain the quantitative dependence for the positions of ionization and acceleration zones on wall properties, a simple 1D stationary model was developed. It was shown that the difference in the electron–wall collision frequency for BGP and BN-05 caused the increase of electron conductivity in the latter case with the shift of ionization frequency and electric field maximum to the anode. The difference in electron–wall collision frequencies was caused by different emission yields of secondary electrons at BGP and BN-05 walls.

REFERENCES

1. Garnier, Y., J.-F. Roussel, and D. Pagnon. 1999. Investigation of xenon ion sputtering of one ceramic material used in SPT discharge chamber. *26th Electric Propulsion Conference (International) Proceedings*. Kitakyushu. IEPC-99-083.
2. Peterson, P. Y., and D. H. Manzella. 2003. Investigation of the erosion characteristics of a laboratory Hall thruster. AIAA Paper No. 2003-5005.
3. Gascon, N., M. Dudeck, and S. Barral. 2003. Wall material effects in stationary plasma thrusters. *Phys. plasmas* 10(10).
4. Kim, V., V. Kozlov, A. Skrylnikov, A. Veselovzorov, J. M. Fife, and S. C. Locke. 2003. Investigation of operation and characteristics of small SPT with discharge channel walls made of different ceramics. AIAA JPC-2003.
5. Abashkin, V. V., O. A. Gorshkov, A. S. Lovtsov, and A. A. Shagaida. 2007. Analysis of ceramic erosion characteristic in hall-effect thruster with higher specific impulse. *30th Electric Propulsion Conference (International) Proceedings*. Florence, Italy. IEPC-2007-133.
6. Lovtsov, A. S., O. A. Gorshkov, and A. A. Shagayda. 2006. Semi-empirical method of hall thrusters lifetime prediction. AIAA Paper No. 2006-4661.
7. Maslennikov, N. A. 1995. Lifetime of stationary plasma thruster. *24th Propulsion Conference (International) Proceedings*. Moscow, Russia. IEPC-95-75.
8. Belikov, M. B., O. A. Gorshkov, E. N. Dyshlyuk, A. S. Lovtzov, and A. A. Shagayda. 2007. Development of low-power Hall thruster with lifetime up to 3000 hours. *30th Electric Propulsion Conference (International) Proceedings*. Florence, Italy. IEPC-2007-129.
9. Tahara, H., K. Imanaka, and S. Yuge. 2005. Effects of channel wall material on performance and plasma characteristics of Hall thrusters. *29th Propulsion Conference (International) Proceedings*. Princeton University, USA. IEPC-2005-015.

10. Tahara, H., T. Fujioka, A. Shirasaki, and T. Yoshikawa. 2003. Simple one-dimensional calculation of Hall thruster flowfields. *28th Electric Propulsion Conference (International) Proceedings*. Toulouse, France. IEPC-2003-0016-0303.
11. Jolivet, L., and J.-F. Roussel. 2000. Effects of the secondary electron emission on the sheath phenomenon in a Hall thruster. *3rd Conference (International) on Spacecraft Propulsion Proceedings*. Noordwijk, Netherlands: ESA Publication Division.
12. Viel-Inguimbert, V. 2003. Secondary electron emission of ceramics used in the channel of SPT. *28th Electric Propulsion Conference (International), The Electric Rocket Propulsion Society Proceedings*. Worthington, OH. IEPC-03-258.